

Assembly of Lipophilic Tetranuclear (Cu₄ and Zn₄) Molecular Metallophosphonates from 2,4,6-Triisopropylphenylphosphonic Acid and Pyrazole Ligands

Vadapalli Chandrasekhar,* Palani Sasikumar, Ramamoorthy Boomishankar, and Ganapathi Anantharaman

Department of Chemistry, Indian Institute of Technology, Kanpur-208016, India

Received January 2, 2006

A sterically hindered aryl phosphonic acid ArP(O)(OH)₂ (**2**) (Ar = 2,4,6-isopropylphenyl) was synthesized and structurally characterized. ArP(O)(OH)₂ forms an interesting hydrogen-bonded *corrugated sheet*-type supramolecular structure in the solid-state. A three-component reaction involving ArP(O)(OH)₂, 3,5-dimethylpyrazole(DMPZH), and Cu(CH₃COO)₂·2H₂O produces the tetranuclear Cu(II) compound [Cu₄(μ₃-OH)₂{ArPO₂(OH)}₂(CH₃CO₂)₂(DMPZH)₄][CH₃COO]₂·CH₂Cl₂ (**3**). A similar three-component reaction involving ArP(O)(OH)₂, 3,5-dimethylpyrazole, and Zn(CH₃COO)₂·2H₂O yields the tetranuclear Zn(II) compound [Zn₄{ArPO₃}₂{ArPO₂(OH)}₂{DMPZH}₄(DMPZ)₂·5MeOH (**4**). While **3** has been found to have an asymmetric cage structure where two dinuclear copper cores are bridged by bidentate [ArPO₂(OH)]⁻ ligands, **4** possesses an *open-book* tricyclic structure composed of three fused metallophosphonate rings. Magnetic studies on **3** revealed antiferromagnetic behavior.

Introduction

The use of organophosphonic acids as ligands in transition metal chemistry is well established for the preparation of metal phosphonates that possess extended layered and pillared structures.¹ The utility of such metal phosphonates in applications ranging from catalysis to sorption is well documented.¹ In contrast to the widespread use of phosphonate ligands in the preparation of compounds with extended structures, their application in the preparation of molecular compounds containing main-group and transition metals is more recent.^{2–7} We have shown that phosphonic acids, in conjunction with ancillary ligands such as pyrazole, are extremely effective for the preparation of soluble molecular multimetal phosphonates. Thus, for example, we have been

able to isolate dodecanuclear^{3a} and decanuclear^{3b} copper(II) clusters in a three-component reaction involving a Cu(II) salt, *tert*-butylphosphonic acid, and pyrazole ligands. This procedure can be adapted for the synthesis of other types of

* To whom correspondence should be addressed. Phone: 91-512-2597259. Fax: 91-512-2590007/2597436. E-mail: vc@iitk.ac.in.

- (1) (a) Clearfield, A. *Prog. Inorg. Chem.* **1998**, *47*, 371. (b) Inoue, A.; Shinokubo, H.; Oshima, K. *J. Am. Chem. Soc.* **2003**, *125*, 1484. (c) Deniaud, D.; Schollorn, B.; Mansury, J.; Rouxel, J.; Battion, P.; Bujoli, B. *Chem. Mater.* **1995**, *7*, 995. (d) Ouellette, W.; Golub, V.; Connor, C. J. O.; Zubieta, J. *Dalton Trans.* **2005**, 291. (e) Finn, R. C.; Zubieta, J. *Chem. Commun.* **2000**, 1321. (f) Fredouel, F.; Massiot, D.; Janvier, P.; Gingl, F.; Doeuff, M. B.; Evian, M.; Clearfield, A.; Bujoli, B. *Inorg. Chem.* **1999**, *38*, 1831. (g) Ouelette, W.; Koo, B. K.; Burkholder, E.; Golub, V.; Connor, C. J. O.; Zubieta, J. *Dalton Trans.* **2004**, 1527. (h) Khan, I.; Zubieta, J. *Prog. Inorg. Chem.* **1995**, *43*, 1. (2) (a) Walawalkar, M. G.; Roesky, H. W.; Murugavel, R. *Acc. Chem. Res.* **1999**, *32*, 117. (b) Chandrasekhar, V.; Gopal, K. *Appl. Organomet. Chem.* **2005**, *19*, 429.

- (3) (a) Chandrasekhar, V.; Kingsley, S. *Angew. Chem., Int. Ed.* **2000**, *39*, 2320. (b) Chandrasekhar, V.; Nagarajan, L.; Gopal, K.; Baskar, V.; Kögerler, P. *Dalton Trans.* **2005**, 3143. (c) Chandrasekhar, V.; Kingsley, S.; Vij, A.; Lam, K. C.; Rheingold, A. L. *Inorg. Chem.* **2000**, *39*, 3238. (d) Clarke, R.; Latham, K.; Rix, C.; Hobday, M.; White, J. *CrystEngComm* **2005**, *7*, 28. (e) Clarke, R.; Latham, K.; Rix, C.; Hobday, M.; White, J. *CrystEngComm* **2004**, *6*, 42. (4) (a) Chandrasekhar, V.; Kingsley, S.; Hatigan, B.; Lam, M. K.; Rheingold, A. L. *Inorg. Chem.* **2002**, *41*, 1030. (b) Anantharaman, G.; Chandrasekhar, V.; Walawalkar, G. W.; Roesky, H. W.; Vidovic, D.; Magull, J.; Nottlemeyer, M. *Dalton Trans.* **2004**, 1271. (c) Cao, D. K.; Li, Y. Z.; Zheng, L. M. *Inorg. Chem.* **2005**, *44*, 2984. (d) Rao, C. N. R.; Natarajan, S.; Choudhury, A.; Neeraj, S.; Ayi, A. A. *Acc. Chem. Res.* **2001**, *34*, 80. (5) (a) Mason, M. R.; Perkins, A. M.; Matthews, R. M.; Fisher, J. D.; Mashuta, M. S.; Vij, A. *Inorg. Chem.* **1998**, *37*, 3734. (b) Cao, D. K.; Li, Y. Z.; Song, Y.; Zheng, L. M. *Inorg. Chem.* **2005**, *44*, 3599. (c) Lei, C.; Mao, J.; Sun, Y.; Zeng, H.; Clearfield, A. *Inorg. Chem.* **2003**, *42*, 6157. (d) Fan, Y.; Li, G.; Jian, W.; Yu, M.; Wang, L.; Tian, Z.; Song, T.; Feng, S. *J. Solid State Chem.* **2005**, *178*, 2267. (6) (a) Chandrasekhar, V.; Baskar, V.; Steiner, A.; Zacchini, S. *Organometallics* **2002**, *21*, 4528. (b) Chandrasekhar, V.; Baskar, V.; Vittal, J. J. *Am. Chem. Soc.* **2003**, *125*, 2392. (7) (a) Langley, S. J.; Helliwell, M.; Sessoli, R.; Rosa, P.; Wernsdorfer, W.; Winpenny, R. E. P. *Chem. Commun.* **2005**, 5029. (b) Tolis, E. I.; Helliwell, M.; Langley, S.; Raftery, J.; Winpenny, R. E. P. *Angew. Chem., Int. Ed.* **2003**, *42*, 2556. (c) Maheswaran, S.; Chastanet, G.; Teat, S. J.; Mallah, T.; Sessoli, R.; Wernsdorfer, W.; Winpenny, R. E. P. *Angew. Chem., Int. Ed.* **2005**, *44*, 5044.

metal phosphonate clusters as well.^{4a,7a} To assess the role of a sterically hindered aryl phosphonic acid on the nuclearity of the metal assembly, as well as its eventual architecture, we have studied the reactions of 2,4,6-triisopropylphenylphosphonic acid with Cu(II) and Zn(II) salts in the presence of ancillary pyrazole ligands. For this purpose we have synthesized $\text{ArP}(\text{O})(\text{OH})_2$ (**2**) from $\text{ArP}(\text{O})\text{Cl}_2$ (**1**). Here, we report the synthesis and structural characterization of **1** and **2**. It may be mentioned that structural studies of aryl phosphonic acids are limited.⁸ The lipophilic arylphosphonic acid prepared in this study, $\text{ArP}(\text{O})(\text{OH})_2$ (**2**), forms an interesting hydrogen-bonded *corrugated sheet*-type supramolecular structure in the solid-state. We report that $\text{ArP}(\text{O})(\text{OH})_2$ (**2**) can be used in combination with 3,5-dimethylpyrazole to produce $[\text{Cu}_4(\mu_3\text{-OH})_2\{\text{ArPO}_2(\text{OH})\}_2(\text{CH}_3\text{CO}_2)_2\text{-}(\text{DMPZH})_4]\cdot 2(\text{CH}_3\text{CO}_2)\cdot \text{CH}_2\text{Cl}_2$ (**3**) and $[\text{Zn}_4\{\text{ArPO}_3\}_2\text{-}\{\text{ArPO}_2(\text{OH})\}_2\{\text{DMPZH}\}_4(\text{DMPZ})_2]\cdot 5\text{CH}_3\text{OH}$ (**4**) (DMPZH = 3,5-dimethylpyrazole) in nearly quantitative yields. The X-ray crystal structures of **3** and **4** reveal an unprecedented asymmetric cage structure for the former and an *open-book* tricyclic structure for the latter. The structure of the latter is reminiscent of the basic building unit of a one-dimensional ladder zinc phosphate.^{4d}

Experimental Section

General Methods. Solvents and other general reagents used in this work were purified according to standard procedures. 3,5-Dimethylpyrazole⁹ (DMPZH) and 2,4,6-triisopropylphenyl bromide¹⁰ were prepared according to literature procedures. The synthesis of 1,3,5-triisopropylbenzene reported in this work is an adaptation of the synthesis of 1,3,5-tri-*tert*-butylbenzene in the literature.¹¹ Copper(II) acetate monohydrate (Fluka, Switzerland) and zinc(II) acetate dihydrate (SD Fine Chemicals, Mumbai, India) were used without any further purification.

Instrumentation. Melting points were measured using a JSGW melting point apparatus and are uncorrected. Elemental analyses were carried out using a Thermoquest CE instruments model EA/110 CHNS—O elemental analyzer. ¹H and ³¹P NMR spectra were obtained on a JEOL-JNM LAMBDA 400 model spectrometer operating at 400.0 and 161.7 MHz, respectively. The spectra were recorded in CDCl_3 solution, and the chemical shifts were referenced with respect to tetramethylsilane (¹H) and 85% H_3PO_4 (³¹P), respectively. Mass spectra were recorded on a JEOL SX 102/DA 6000 mass spectrometer using xenon (6 kV, 10 mA) as the FAB gas. IR spectra were recorded as KBr pellets on a Bruker Vector 22 FTIR spectrophotometer operating from 400 to 4000 cm^{-1} . Electronic spectra were recorded on Perkin-Elmer Lambda 20 UV-vis spectrometer and on a Shimadzu UV-160 spectrometer using CH_3CN as the solvent. Magnetic susceptibility measurement was carried out by SQUID (superconducting quantum interference device) using a Quantum Design Magnetic property measurement

system XL (U.S.A.) between 313 and 18 K. Magnetic susceptibility was corrected for the magnetization of the sample holder and capsule and the diamagnetic contribution to the samples which were estimated from Pascal's constants. Thermogravimetric analysis curves were obtained on a Perkin-Elmer Pyris6 thermogravimetry analyzer under zero-grade dry nitrogen atmospheres.

X-ray Crystallography. The crystal data for compounds **1–4** were collected on a Bruker SMART APEX CCD Diffractometer. SMART (version 6.45) was used for integration of the intensity of reflections and scaling, and SADABS was used for absorption correction. Empirical absorption corrections were applied for **3** by Xabs2.^{12a} The crystal structures were solved and refined by full-matrix least-squares methods against F^2 using SHELXTL (version 6.14).^{12b} All non-hydrogen atoms were refined with anisotropic displacement parameters. Hydrogen positions were fixed at calculated positions and refined isotropically. Crystal data for **1–4** are given in Table 1.

Synthesis of 1,3,5-Triisopropylbenzene. 2-Bromopropane (762.7 g, 6.24 mol) was added to benzene (121.9 g, 1.56 mol) in a 2 L flask at $-40\text{ }^\circ\text{C}$. Pulverized anhydrous aluminum chloride (417.0 g, 3.12 mol) was added to this mixture in small portions over a period of 2 h. After the complete addition of aluminum chloride, the reaction mixture was allowed to warm to room temperature. During this time vigorous evolution of hydrogen chloride occurred. After the cessation of hydrogen chloride evolution, the reaction mixture was stirred for a further 12 h. Finally, the entire reaction mixture was poured into crushed ice (2 L) in a well-ventilated hood. The organic layer was extracted with diethyl ether (1 L). Removal of diethyl ether, followed by distillation of the residue (0.02 mm, $90\text{--}93\text{ }^\circ\text{C}$), yielded the title compound (302 g, 95% yield). ¹H NMR (400 MHz, CDCl_3 , TMS): δ 1.3 (d, 18H, $\text{CH}(\text{CH}_3)_2$), 2.9 (sept, 1H, $\text{CH}(\text{CH}_3)_2$), 7.0 (d, 2H, aromatic).

Synthesis of 2,4,6-Triisopropylphenylphosphonous Dichloride, $\text{ArP}(\text{O})\text{Cl}_2$. A literature procedure for the synthesis of $\text{ArP}(\text{O})\text{Cl}_2$ was carried out via the reaction of ArLi with PCl_3 .¹⁰ We have found the Grignard route outlined here to be more convenient. A Grignard solution of 2,4,6-triisopropylphenylmagnesium bromide was prepared by the reaction of 2,4,6-triisopropylphenyl bromide (20 g, 70.6 mmol) with Mg (1.69 g, 70.8 mmol) in 200 mL of dry THF. A few drops of 1,2-dibromoethane was required to initiate the reaction. The Grignard solution was added slowly via cannula to a solution containing PCl_3 (9.7 g, 70.6 mmol) cooled to $-40\text{ }^\circ\text{C}$. After the addition was completed, a solution of anhydrous ZnCl_2 (19.2 g, 141.0 mmol) was added to the reaction mixture. The reaction mixture was stirred for 12 h at $-40\text{ }^\circ\text{C}$. Then it was allowed to come to room temperature and was stirred for 6 h. The reaction mixture was filtered, and the filtrate was stripped off the solvent and other volatile components in vacuo to give a pale yellow viscous oil. This was dissolved in diethyl ether (200 mL) and filtered. Removal of solvent from the filtrate yielded a solid residue which was washed twice with 20 mL of pentane and dried (26.5 g, 81%).

Synthesis of 2,4,6-Triisopropylphenylphosphonic Dichloride, $\text{ArP}(\text{O})\text{Cl}_2$ (1**).** The synthesis of **1** was carried out by adapting a literature procedure.¹⁰ Sulfuryl chloride (9.26 g, 0.07 mol) was added dropwise to a solution of $\text{ArP}(\text{O})\text{Cl}_2$ (19.42 g, 0.64 mol) in carbon tetrachloride (50 mL) at $0\text{ }^\circ\text{C}$. After the addition was complete, the reaction mixture was allowed to attain room temperature and was stirred for 1 h. Removal of the solvent and other volatiles from this reaction mixture in vacuo afforded a white

(8) (a) Mehring, M.; Schürmann, M.; Ludwig, R. *Chem.—Eur. J.* **2003**, *9*, 837. (b) Weakley, T. J. R. *Acta Crystallogr.* **1976**, *B32*, 2889. (c) Aragoni, M. C.; Arca, M.; Blake, A. J.; Lippolis, V.; Schröder, M.; Wilson, C. *Acta Crystallogr.* **2002**, *C58*, 260. (d) Steven, R.; Henderson, W. *J. Organomet. Chem.* **2001**, *637–639*, 216.
 (9) Furniss, B. S.; Hannaford, A. J.; Smith, P. W. G.; Tatchell, A. R. *Vogel's Text Book of Practical Organic Chemistry*, 5th ed.; ELBS and Longman: London, 1989.
 (10) Whitesides, G. M.; Eisenhut, M.; Bunting, W. M. *J. Am. Chem. Soc.* **1974**, *96*, 5399.
 (11) Pearson, D. E.; Buehler, C. A. *Synthesis*. **1971**, 455.

(12) (a) Parkin, S.; Moezzi, B.; Hope, H. *J. Appl. Crystallogr.* **1995**, *28*, 53. (b) Scheldrick, G. M. *SHELXL-97, Program for Crystal Structure Analysis*, release 97-2; University of Göttingen: Göttingen, Germany, 1998.

Table 1. Crystal Data and Structure Refinement Parameters for (1–4)

	ArPOCl ₂ (1)	ArPO ₃ H ₂ (2)	Cu ₄ (3)	Zn ₄ (4)
empirical formula	C ₁₅ H ₂₃ Cl ₂ O ₁ P ₁	C ₁₅ H ₂₅ O ₃ P ₁	C ₅₉ H ₉₄ N ₈ O ₁₆ P ₂ Cl ₂ Cu ₄	C ₉₅ H ₁₆₀ N ₁₂ O ₁₇ P ₄ Zn ₄
fw	320.25	284.33	1554.43	2127.81
temp	100(2) K	100(2) K	100(2) K	293(2) K
wavelength	0.71073 Å	0.71073 Å	0.71073 Å	0.71073 Å
cryst syst	monoclinic	monoclinic	triclinic	triclinic
space group	<i>P</i> 1	<i>P</i> 2 ₁ / <i>n</i>	<i>P</i> 1	<i>P</i> 1
unit cell dimensions	<i>a</i> = 9.720(7) Å <i>b</i> = 14.397(8) Å <i>c</i> = 11.649(4) Å α = 90.000° β = 95.558(10)° γ = 90.000°	<i>a</i> = 16.624(3) Å <i>b</i> = 6.067(7) Å <i>c</i> = 16.728(5) Å α = 90.000° β = 110.597(10)° γ = 90.000°	<i>a</i> = 12.4542(19) Å <i>b</i> = 13.852(2) Å <i>c</i> = 22.939(4) Å α = 86.679(3)° β = 89.099(3)° γ = 88.595(3)°	<i>a</i> = 15.898(5) Å <i>b</i> = 16.563(5) Å <i>c</i> = 21.746(5) Å α = 95.366(5)° β = 101.054(5)° γ = 103.679(5)°
vol	1622.75(14) Å ³	1579.6(2) Å ³	3949.3(10) Å ³	5402(3) Å ³
Z	4	4	2	2
density calcd	1.339 Mg/m ³	1.187 Mg/m ³	1.277 Mg/m ³	1.259 Mg/m ³
abs coeff	0.490 mm ⁻¹	0.176 mm ⁻¹	1.197 mm ⁻¹	0.997 mm ⁻¹
<i>F</i> (000)	704	608	1586	2170
crystal size	0.2 × 0.1 × 0.1 mm ³	0.2 × 0.1 × 0.1 mm ³	0.2 × 0.2 × 0.2 mm ³	0.2 × 0.1 × 0.1 mm ³
θ range	2.10–28.31°	2.15–28.30°	2.18–24.71°	4.08–22.49°
limiting indices	–12 ≤ <i>h</i> ≤ 12 –16 ≤ <i>k</i> ≤ 19 –15 ≤ <i>l</i> ≤ 14	–22 ≤ <i>h</i> ≤ 19 –8 ≤ <i>k</i> ≤ 8 –22 ≤ <i>l</i> ≤ 17	–14 ≤ <i>h</i> ≤ 14 –16 ≤ <i>k</i> ≤ 16 0 ≤ <i>l</i> ≤ 26	–16 ≤ <i>h</i> ≤ 17 –15 ≤ <i>k</i> ≤ 17 –23 ≤ <i>l</i> ≤ 23
reflns collected/unique	10 620/3989 [<i>R</i> (int) = 0.0145]	10 004/3893 [<i>R</i> (int) = 0.0283]	13 240/13240 [<i>R</i> (int) = 0.0000]	22 736/1394 [<i>R</i> (int) = 0.0563]
completeness to θ	98.8% (θ = 28.31°)	99.3% (θ = 28.30°)	98.2% (θ = 24.71°)	98.9% (θ = 22.49°)
abs correction	not applied	not applied	empirical	semiempirical
refinement method	full-matrix least-squares on <i>F</i> ²	full-matrix least-squares on <i>F</i> ²	full-matrix least-squares on <i>F</i> ²	full-matrix least-squares on <i>F</i> ²
data/restraints/params	3989/0/178	3893/0/186	13 240/0/848	13 949/34/1170
GOF on <i>F</i> ²	1.078	1.067	1.030	1.039
final <i>R</i> indices [<i>I</i> > 2 σ (<i>I</i>)]	<i>R</i> 1 = 0.0307 <i>wR</i> 2 = 0.0814	<i>R</i> 1 = 0.0508 <i>wR</i> 2 = 0.1309	<i>R</i> 1 = 0.0699 <i>wR</i> 2 = 0.1863	<i>R</i> 1 = 0.0771 <i>wR</i> 2 = 0.1648
<i>R</i> indices (all data)	<i>R</i> 1 = 0.0326 <i>wR</i> 2 = 0.0826	<i>R</i> 1 = 0.0597 <i>wR</i> 2 = 0.1369	<i>R</i> 1 = 0.0930 <i>wR</i> 2 = 0.1975	<i>R</i> 1 = 0.1206 <i>wR</i> 2 = 0.1856
largest diff. peak and hole	0.444 and –0.236 e Å ⁻³	0.948 and –0.264 e Å ⁻³	1.873 and –0.629 e Å ⁻³	0.772 and –0.474 e Å ⁻³

precipitate which was washed twice with *n*-hexane (5 mL) and dried (7.2 g, 68%). Further purification of this compound was achieved by recrystallization (diethyl ether/*n*-pentane mixture (4:1), 0 °C). ³¹P NMR (CDCl₃): δ 33.5 (s).

Preparation of 2,4,6-Trisopropylphenylphosphonic Acid, ArP(O)(OH)₂ (2). A sodium hydroxide solution (2.0 g in 100 mL) was added to a solution of **1** (2.0 g, 6.25 mmol) in acetone (70 mL), and the reaction mixture was stirred at room temperature for 48 h. The mixture was extracted with dichloromethane, and the organic layer was evaporated to produce a white solid which was identified as ArP(O)(OH)₂ (**2**). Recrystallization of **2** was carried out from a mixture of petroleum ether (40–60 °C) and toluene (1:1) at room temperature. Yield: 1.65 g (95%). mp: 174–176 °C. Anal. Calcd for C₁₅H₂₅O₃P (284.33): C, 63.36; H, 8.86. Found: C, 62.94; H, 7.90. ¹H NMR (399.65 MHz, CDCl₃, TMS): δ 1.22 (d, 18H, *J*(¹H–¹H) = 6.9 Hz), *o*-CH(CH₃)₂, 2.87 (sept, 2H, *J*(¹H–¹H) = 6.9 Hz), *p*-CH(CH₃)₂, 3.99 (sept, 1H, *J*(H,H) = 6.7 Hz), 7.11 (d, 2H, aromatic), 10.53 (br, 2H, OH). ³¹P NMR (CDCl₃): δ 28.3 (s). ESI-MS: *m/z* 284 (C₁₅H₂₅PO₃, 86%), 269 (C₁₄H₂₂O₃P, 100%). IR (CH₂Cl₂, cm⁻¹): 3944 (s), 3756 (s), 3692 (s), 3598 (w), 3535 (w), 2982 (s), 2686 (s), 2523 (s), 2411 (s), 2305 (s), 2155 (m), 2055 (m), 2001 (w), 1887 (w), 1785 (w), 1712 (w), 1602 (s), 1551 (s), 1459 (s), 1291 (s), 1242 (vs), 993 (s), 893 (s), 764 (s), 687 (s). IR (KBr, cm⁻¹): 2960 (vs), 2316 (m), 1605 (m), 1558 (m), 1460 (m), 1425 (m), 1365 (m), 1182(s), 994(s), 942(m), 908(s), 794(m), 652 (s), 579(s), 531(s), 500(s).

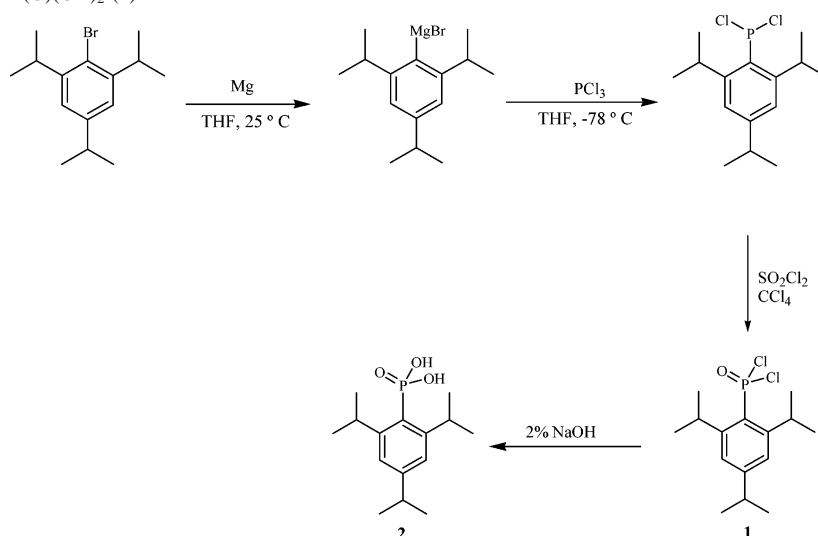
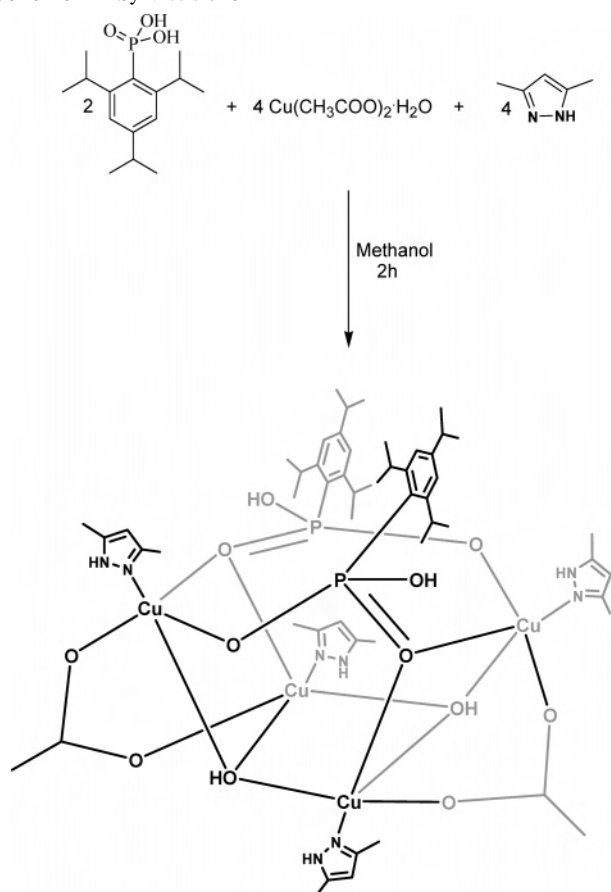
Preparation of [Cu₄(μ_3 -OH)₂{(ArP(O)₂(OH))₂(CH₃CO₂)₂-(DMPZH)₄]-[(CH₃CO₂)₂]-CH₂Cl₂ (3). 3,5-Dimethylpyrazole (0.07 g, 0.73 mmol) was added to a suspension of copper(II) acetate monohydrate (0.14 g, 0.70 mmol) in methanol (50 mL), and the resultant deep green reaction mixture was stirred for 5 min. At this stage, ArP(O)(OH)₂ (0.10 g, 0.35 mmol) was added to this reaction

mixture all at once. The color of the reaction mixture changed to light green. It was allowed to stir at room temperature for 2 h. Removal of methanol in vacuo yielded a blue solid. This was recrystallized by allowing *n*-hexane to diffuse in to its dichloromethane solution at room temperature. Yield: 0.26 g (96%). mp: 172–174 °C. Anal. Calcd for C₅₉H₉₆N₈O₁₆P₂Cl₂Cu₄ (1554.28): C, 45.41; H, 6.20; N, 7.18. Found: C, 44.70; H, 6.23; N, 6.80. UV–vis (CH₃OH): λ_{\max} 666 nm (ϵ = 146.59 L mol⁻¹ cm⁻¹). μ (per one copper): 0.91 (303 K), 0.47 (18 K). IR (KBr, cm⁻¹): 3267 (m), 2955 (s), 1575 (s), 1428 (s), 1262 (s), 1094 (vs), 1018 (vs), 868 (m), 802 (vs), 655 (m), 544 (m).

Preparation of [Zn₄(ArPO₃)₂{(ArP(O)₂(OH))₂(DMPZH)₄-(DMPZ)₂]-5CH₃OH (4). 3,5-Dimethylpyrazole (0.05 g, 0.53 mmol) was added to a suspension of zinc(II)acetate dihydrate (0.08 g, 0.36 mmol) in methanol (50 mL), and the mixture was stirred for 5 min. At this stage, ArP(O)(OH)₂ (0.10 g, 0.35 mmol) was added. The reaction mixture was stirred for 2 h, concentrated to 5 mL, and kept for crystallization at 0 °C. Yield: 0.19 g (98%). mp: 206–208 °C. Anal. Calcd for C₉₅H₁₆₀N₁₂O₁₇P₄Zn₄ (2120.81): C, 53.62; H 7.58; N, 7.90. Found: C, 54.01, H 7.14, N, 7.41. ³¹P NMR: δ 13.5 (s), 18.5 (s). IR (KBr, cm⁻¹): 3314 (s), 2956 (s), 2869 (s), 1596 (s), 1427 (s), 1315 (s), 1109 (s, sh), 1077 (vs), 986 (s), 879 (m), 784 (m), 710 (m), 657 (s), 551 (s).

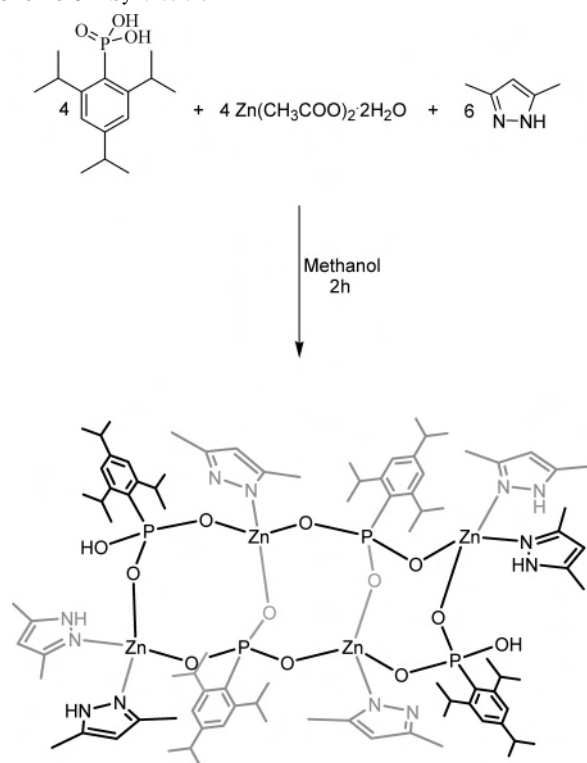
Results and Discussion

Synthetic Aspects. The synthesis of the ArP(O)(OH)₂ (**2**) is outlined in Scheme 1. The synthetic procedure consists of first converting the arylphosphonous dichloride, ArPCL₂, to the arylphosphonic dichloride, ArP(O)Cl₂ (**1**) by treatment with SO₂Cl₂. Compound **1** is hydrolyzed using a strong base to afford the lipophilic phosphonic acid, ArP(O)(OH)₂ (**2**)

Scheme 1. Synthesis of $\text{ArP(O)}_2(\text{OH})_2$ (**2**)**Scheme 2.** Synthesis of **3**^a

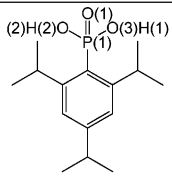
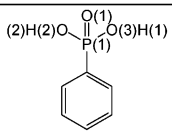
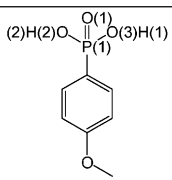
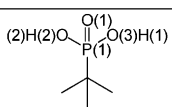
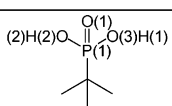
^a The acetate anions present in the molecule are not shown.

in an excellent yield (vide supra, experimental). The conversion of **1** to **2** is accompanied by an upfield chemical shift in the ^{31}P NMR spectra (33.5 (**1**) and 28.3 ppm (**2**)). The EI mass spectrum of **2** shows the molecular ion peak at 284. The arylphosphonic acid, **2**, is an air stable lipophilic solid which can be readily used as a synthon for the preparation of metallophosphonates. Thus, the reaction of **2** with $\text{Cu}(\text{OAc})_2 \cdot \text{H}_2\text{O}$ or $\text{Zn}(\text{OAc})_2 \cdot 2\text{H}_2\text{O}$ in the presence of 3,5-dimethylpyrazole at ambient temperature affords the tetra-

Scheme 3. Synthesis of **4**

nuclear compounds $[\text{Cu}_4(\mu_3\text{-OH})_2\{\text{ArP(O)}_2(\text{OH})\}_2(\text{CH}_3\text{CO}_2)_2(\text{DMPZH})_4][\text{CH}_3\text{COO}]_2 \cdot \text{CH}_2\text{Cl}_2$ (**3**) and $[\text{Zn}_4(\text{ArPO}_3)_2\{\text{ArP(O)}_2(\text{OH})\}_2(\text{DMPZH})_4(\text{DMPZ})_2] \cdot 5\text{MeOH}$ (**4**) in nearly quantitative yields (Schemes 2 and 3). The ^{31}P NMR of **4** shows two singlets at 13.5 and 18.5 ppm consistent with its molecular structure which shows the presence of both the monoanionic $\text{RPO}_2(\text{OH})$ and the dianionic RPO_3 ligands. Thermogravimetric analysis of **3** and **4** were carried out to ascertain the thermal stability of these tetranuclear clusters. Although the weight loss for these compounds starts at fairly low temperatures, the final decomposition occurs at 399.9 (**3**, residue 27.3%) and 479.5 °C (**4**, residue 32.2%) (see Supporting Information for TGA traces). Infrared spectrum of the phosphonic acid, **2**, in the solid-state reveals a strong

Table 2. Comparison of the Structural Parameters in the Molecular and Crystal Structures of ArP(O)(OH)₂ with Some Related Derivatives

S. no	phosphonic acid	bond		hydrogen-bonded structure	O...O distances and angles between adjacent molecule	ref
		distances (Å)	angle (deg)			
1		P(1)-O(1) 1.506(8) P(1)-O(2) 1.553(6) P(1)-O(3) 1.561(5) P(1)-C(1) 1.799(0)	O(1)-P(1)-O(2) 112.5(7) O(1)-P(1)-O(3) 109.3(8) O(2)-P(1)-O(3) 105.6(6) O(1)-P(1)-C(1) 113.9(3) O(2)-P(1)-C(1) 108.7(3) O(3)-P(1)-C(1) 106.1(8)	corrugated sheet	O(3)...O(1') 2.582(1) O(2)...O(1'') 2.613(7) O(3)-H(1)-O(1') 174.2(6) O(2)-H(2)-O(1'') 172.2(5)	this paper
2		P(1)-O(1) 1.496(4) P(1)-O(2) 1.550(4) P(1)-O(3) 1.539(3) P(1)-C(1) 1.773(5)	O(1)-P(1)-O(2) 112.1(2) O(1)-P(1)-O(3) 111.3(2) O(2)-P(1)-O(3) 106.9(2) C(1)-P(1)-O(1) 110.7(2) C(1)-P(1)-O(2) 108.3(2) C(1)-P(1)-O(3) 107.4(2)	two-dimensional layer	O(3)...O(1') 2.554(6) O(2)...O(1'') 2.608(5) O(3)-H(1)-O(1') 169.1(2) O(2)-H(2)-O(1'') 169.1(2)	8b
3		P(1)-O(1) 1.511(2) P(1)-O(2) 1.557(2) P(1)-O(3) 1.552(2) P(1)-C(1) 1.771(3)	O(1)-P(1)-O(2) 112.0(3) O(1)-P(1)-O(3) 109.8(8) O(2)-P(1)-O(3) 110.1(2) C(1)-P(1)-O(1) 110.9(7) C(1)-P(1)-O(2) 105.9(6) C(1)-P(1)-O(3) 107.7(3)	helical structure	O(2)...O(1') 2.580(3) O(3)...O(1'') 2.550(3) O(2)-H(2)-O(1') 169 O(3)-H(1)-O(1') 169	8c
4		P(1)-O(1) 1.506(2) P(1)-O(2) 1.557(2) P(1)-O(3) 1.542(2)	O(1)-P(1)-O(2) 105.1(4) O(1)-P(1)-O(3) 112.2(3) O(2)-P(1)-O(3) 110.2(9) O(1)-P(1)-C(1) 105.5(7) O(2)-P(1)-C(1) 108.3(5) O(3)-P(1)-C(1) 112.0(2)	corrugated sheet	O(2)...O(1') 2.579(1) O(3)...O(1'') 2.645(5) O(2)-H(2)-O(1') 175.5(9) O(3)-H(1)-O(1') 175.7(8)	8a
5		P(1)-O(1) 1.508(3) P(1)-O(2) 1.554(4) P(1)-O(3) 1.544(8)	O(1)-P(1)-O(2) 110.7(0) O(1)-P(1)-O(3) 112.4(1) O(2)-P(1)-O(3) 110.2(9) O(1)-P(1)-C(1) 112.3(1) O(2)-P(1)-C(1) 105.7(4) O(3)-P(1)-C(1) 105.0(5)	hexameric cage	O(2)...O(1') 2.596(2) O(3)...O(1'') 2.541(2) O(2)-H(2)-O(1') 177.3 O(3)-H(1)-O(1') 175.3	8a

peak at 1182 cm⁻¹ which is assigned to the P=O stretching frequency on the basis of literature precedents.¹⁴ The O-H stretching frequency could not be observed in the solid-state presumably because of the extensive hydrogen bonding. However, in dichloromethane solution two sharp peaks at 3756 and 3692 cm⁻¹ were seen from the O-H stretch.

Further, the P=O stretching frequency moves to 1242 cm⁻¹ in solution, indicating the loss of hydrogen bonding. The IR spectra of the tetranuclear cages reveal strong peaks at 1094 (ν_{asym} PO₃) and 1018 cm⁻¹ (ν_{sym} PO₃) for **3**. The correspond-

(13) Chandrasekhar, V.; Azhakar, R. *CrystEngComm* **2005**, *7*, 346.

(14) (a) Thomas, L. C.; Chittenden, R. A. *Spectrochim. Acta* **1964**, *20*, 467. (b) Corbridge, D. E. C. *J. Appl. Chem.* **1956**, *6*, 456. (c) Kong, D.; Li, Y.; Ouyang, X.; Prosvirin, A. V.; Zhao, H.; Ross, J. H.; Dunbar, J. K. R.; Clearfield, A. *Chem. Mater.* **2004**, *16*, 3020.

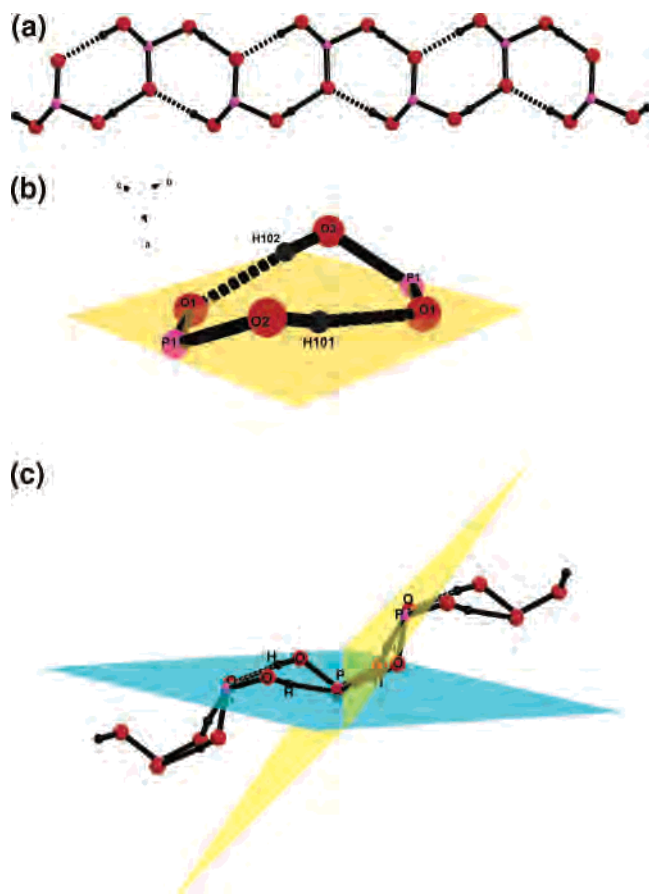


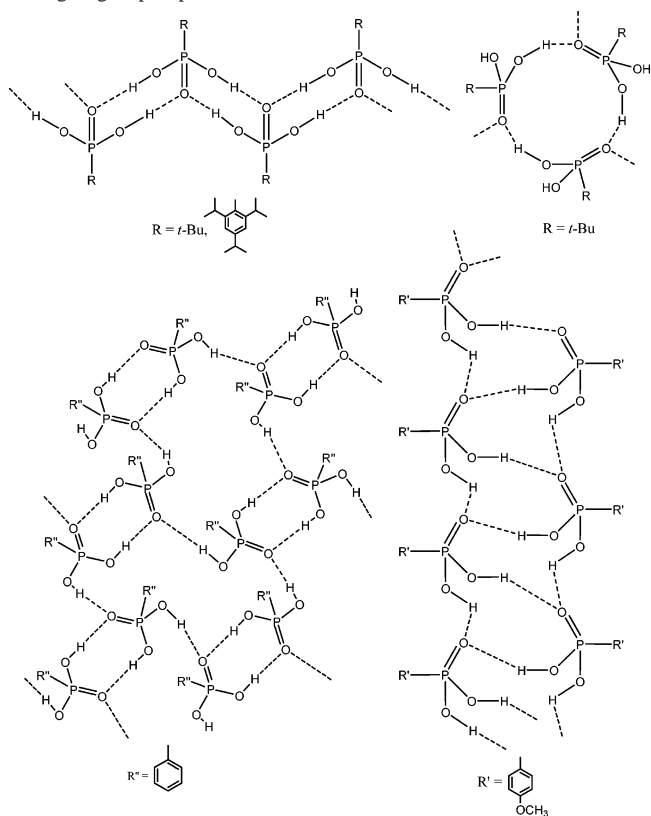
Figure 1. (a) Diamond representation of the intermolecular hydrogen bonding in $\text{ArP}(\text{O})(\text{OH})_2$ (**2**). Color scheme: P, pink; O, red; H, black. (b) A single puckered eight-membered ring of the hydrogen-bonded sheet of **2**; the least-squares plane goes through eight atoms (O1, P1, O3, H102, O1, P1, O2, and H101). Color scheme: P, pink; O, red; H, black. (c) The relative orientation of the adjacent eight-membered rings in the intermolecular hydrogen-bonded sheet of **2**. The least-squares plane goes through eight atoms: plane1 = O1, P1, O2, H101, O1, P1, O3, H102 and plane2 = P1, O1, H102, O3, P1, O1, H101, O2. The angle between plane1 and plane2 is $53.796(3)^\circ$. Color scheme: P, pink; O, red; H, black.

ing peaks for **4** are seen at 1077 and 986 cm^{-1} , respectively (see Supporting Information for IR spectra of **2–4**).

X-ray Crystal Structures of 1–4. The X-ray crystal structures of **1** and **2** confirm their molecular structures (Supporting Information). The bond parameters observed for **1** are quite normal (Supporting Information). The $\text{P}=\text{O}$ distance for **1** is $1.461(9)\text{ \AA}$, and it compares quite well with analogous distances [cf. the $\text{P}=\text{O}$ distance in $\text{P}(\text{O})(\text{N}(\text{Me})\text{NH}_2)_3$ is 1.485 \AA].¹³ The molecular structure of the phosphonic acid, $\text{ArP}(\text{O})(\text{OH})_2$ (**2**), shows three types of $\text{P}-\text{O}$ bond distances (Table 2). The shortest distance is $1.506(13)\text{ \AA}$, and it corresponds to the formal $\text{P}=\text{O}$ present in this compound. The slight lengthening of this $\text{P}=\text{O}$ bond in **2** is the result of the extensive hydrogen bonding which involves this bond (vide infra). Other phosphonic acids where the $\text{P}=\text{O}$ unit is involved in hydrogen bonding also exhibit a similar increase of the $\text{P}=\text{O}$ bond length: $t\text{-BuP}(\text{O})(\text{OH})_2$ ^{8a} (polymeric form), $1.506(2)\text{ \AA}$; $t\text{-BuP}(\text{O})(\text{OH})_2$ ^{8a} (cluster form), $1.508(3)\text{ \AA}$; $\text{PhP}(\text{O})(\text{OH})_2$,^{8b} $1.496(4)\text{ \AA}$; $p\text{-CH}_3\text{OC}_6\text{H}_4\text{P}(\text{O})(\text{OH})_2$,^{8c} $1.511(2)\text{ \AA}$ (Table 2).

Compound **2** forms an intricate hydrogen-bonding network in its solid state (Figure 1). Each phosphonic acid molecule

Chart 1. Supramolecular Structure Mediated by Hydrogen Bonding among Organophosphonic Acids.



simultaneously participates in three hydrogen bonds. The two $\text{P}-\text{O}-\text{H}$ units function as *proton donors* to the two adjacent phosphoryl $\text{P}=\text{O}$ units. The latter functions as a proton acceptor, simultaneously accepting protons from two adjacent molecules. This leads to the formation of a one-dimensional *corrugated sheet*-type structure containing fused eight-membered rings (2P , 4O , and 2H). The phosphoryl units are positioned alternately in the front and back of the sheet (Figure 1, Chart 1). The eight-membered rings present within the sheet are nonplanar. The dihedral angle between adjacent eight-membered rings is about 54° (Figure 1c). The $\text{O}\cdots\text{O}$ distances involved in this intermolecular hydrogen bonding interaction are $2.582(1)$ and $2.613(7)\text{ \AA}$. The $\text{O}-\text{H}\cdots\text{O}$ bond angles are nearly linear: $174.2(6)$ and $172.2(5)^\circ$. These bond parameters are comparable to those observed in other phosphonic acids (Table 2). It is interesting to note that the other phosphonic acid whose structure has been solved recently, $t\text{-BuP}(\text{O})(\text{OH})_2$, crystallizes in two polymorphs.^{8a} One of these polymorphs has a zigzag corrugated sheet structure as described for the present molecule. The other polymorph is a hexameric cluster. The crystal structure of $4\text{-OMe-C}_6\text{H}_4\text{-P}(\text{O})(\text{OH})_2$ reveals a 2D polymeric sheet along a 2_1 screw axis in the unit cell.^{8c} On the other hand the crystal structure of phenylphosphonic acid shows a two-dimensional sheet-type structure.^{8b} The H-bonded situations observed in organophosphonic acids, thus far, are summarized in Chart 1.

The molecular structure of the ionic tetranuclear copper(II) cage, $[\text{Cu}_4(\mu_3\text{-OH})_2\{(\text{ArP}(\text{O})_2(\text{OH}))_2(\text{CH}_3\text{CO}_2)_2\text{-}(\text{DMPZH})_4\}]^{2+}[(\text{CH}_3\text{CO}_2^-)_2\cdot\text{CH}_2\text{Cl}_2]$ (**3**), is shown in Figure

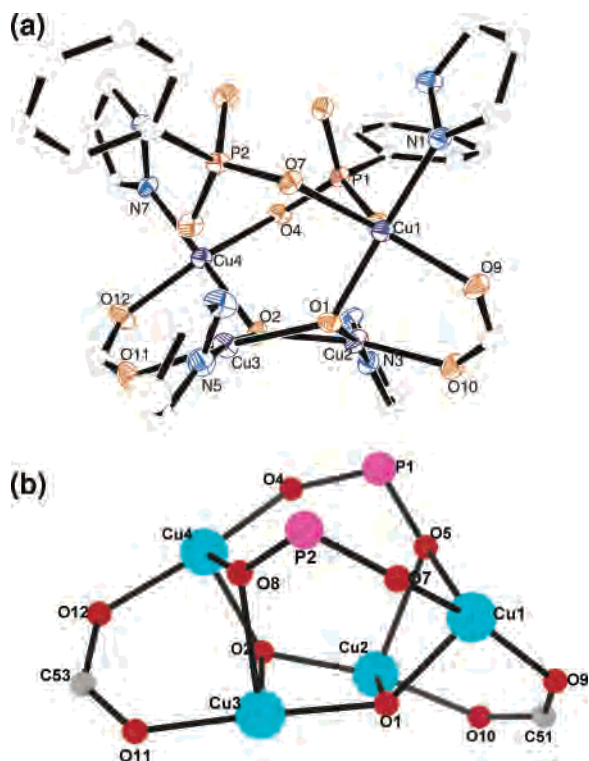
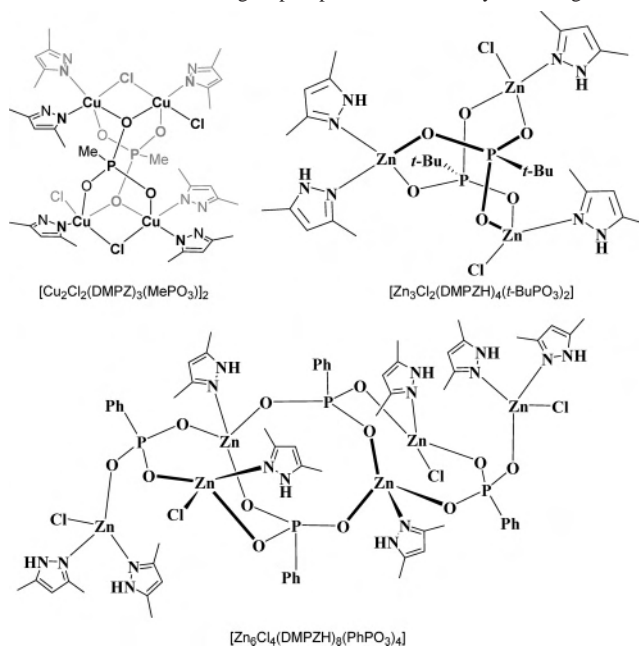


Figure 2. (a) ORTEP diagram of **3** (ellipsoids at 50% probability). The isopropyl substitutions on the phenyl ring, the methyl substitution on the pyrazole rings, the acetate counteranions, the solvent dichloromethane molecule, and the hydrogen atoms are not shown for clarity. Color scheme: Cu, purple; P, orange; O, brown; N, blue; C, gray. (b) The core structure of **3**. Color scheme: Cu, green; P, pink; O, red; C, gray.

2. The molecular structure of **3** can be described as an asymmetric cage containing four copper atoms. The cage possesses a lower narrow rim and an upper wider rim. The lower rim is made up of a four-membered Cu_2O_2 ring, the oxygens being derived from two μ_3 -bridging hydroxyl groups (Figure 2, Scheme 2). The upper rim is wider and is made up of an eight-membered ring (2Cu, 4O, and 2P). Two sides of the cage (opposite sides) contain two four-membered rings (2Cu and 2O) each containing one μ_3 -bridging hydroxyl group and one μ_3 -bridging phosphoryl oxygen. The other two sides of the cage are six-membered rings (2Cu, 3O, and 1P). The overall assembly of the tetranuclear cage, **3**, is assisted by two monoanionic $[\text{RP}(\text{OH})(\text{O})_2]^-$ ligands, two acetate ligands, and two hydroxide ligands. The two $[\text{RP}(\text{OH})(\text{O})_2]^-$ ligands are involved in an asymmetric bridging coordination mode (Cu4–O4, 1.975(4) Å; Cu1–O5, 2.242(4) Å) and form part of the cage structure of the **3** (three types of P–O bond distances are observed for the asymmetric coordinating phosphonate ligand, P1–O–H, 1.534(9) Å; P1–O5, 1.522(4) Å; P1–O4, 1.536(4) Å). It is of interest to note that in an organotin compound, $[(\text{PhCH}_2)_2\text{Sn}_2\text{O}(\text{O}_2\text{P}(\text{OH})-t\text{-Bu})_4]_2$, whose molecular structure was reported by us recently, the phosphonate unit functions as a bridging bidentate ligand also.⁶ In contrast to the asymmetric coordination action of $\text{RP}(\text{OH})(\text{O})_2$ in **3**, the two acetate ligands bind in a nearly symmetric bridging mode (Cu3–O11, 1.957(4) Å; Cu4–O12, 1.966(4) Å) and support the cage structure by their coordination interaction. In addition one oxygen atom of one of the acetate anions has a long-

Chart 2. Schematic Diagram of Tetranuclear Copper and Tri- and Hexanuclear Zinc with Organophosphonic Acid and Pyrazole Ligand



range interaction with the lower-rim copper atoms (2.596(3) and 2.792(2) Å, not shown). All four copper atoms present in **3** are five-coordinate (4O and 1N), although the upper-rim copper atoms (Cu1 and Cu4) and the lower-rim copper atoms (Cu2 and Cu3) form two separate pairs because of the variation of the nature of binding atoms. Every copper atom present in **3** has a neutral pyrazole as a coordinating ligand binding in a monodentate manner. The immediate coordination environment of the upper-rim copper atoms is trigonal bipyramidal with the apical positions being occupied by the hydroxide oxygen atom and the pyrazole nitrogen atom. In contrast the lower-rim copper atoms are in an approximate square-pyramidal geometry (for example, in the coordination environment around Cu2, the basal plane is made up of O1, O2, O10, and N3, while the apical site is occupied by O5, see Supporting Information). It is of interest to compare the molecular structure of **3** with another tetranuclear copper phosphonate cage, $[\text{Cu}_2\text{Cl}_2(3,5\text{-Me}_2\text{Pz})_3(\text{MePO}_3)_2]_2$ ^{3c} (Chart 2). The latter is composed of two independent dinuclear copper cores which are formed and bridged by two tripodal methylphosphonate (MePO_3) ligands. In this case, the two dinuclear copper cores (Cu_2O_2) are fused at the lower rim, and it is only the upper rim that is bridged by the phosphonate coordination action. Despite the structural differences between $[\text{Cu}_2\text{Cl}_2(3,5\text{-Me}_2\text{Pz})_3(\text{MePO}_3)_2]_2$ and **3**, the latter also shows an antiferromagnetic behavior similar to the former. Magnetic measurements on **3** have been carried out from 313 to 18 K. The χ_{MT} versus T plot for **3** is shown in Figure 3. The magnetic moment (spin-only) observed at 303 K is 0.91 μ_{B} per copper. This value drops down to 0.47 at 18 K. This behavior is consistent with the magnetic studies carried out on other copper(II) phosphonates containing pyrazole ancillary ligands.^{3a–3c}

In contrast to the cage structure of **3**, the tetranuclear zinc compound $[\text{Zn}_4(\text{ArPO}_3)_2\{\text{ArP}(\text{O})_2(\text{OH})\}_2(\text{DMPZH})_4(\text{DMPZ})_2]$ (**4**) is a tricyclic compound possessing a novel

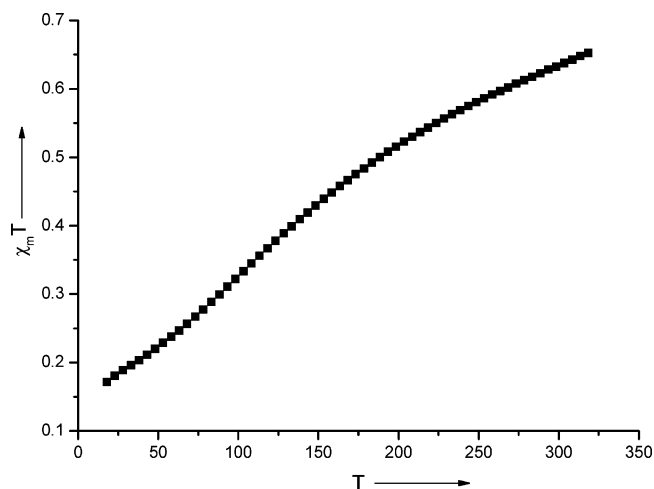


Figure 3. χ_{MT} vs T plot for **3**.

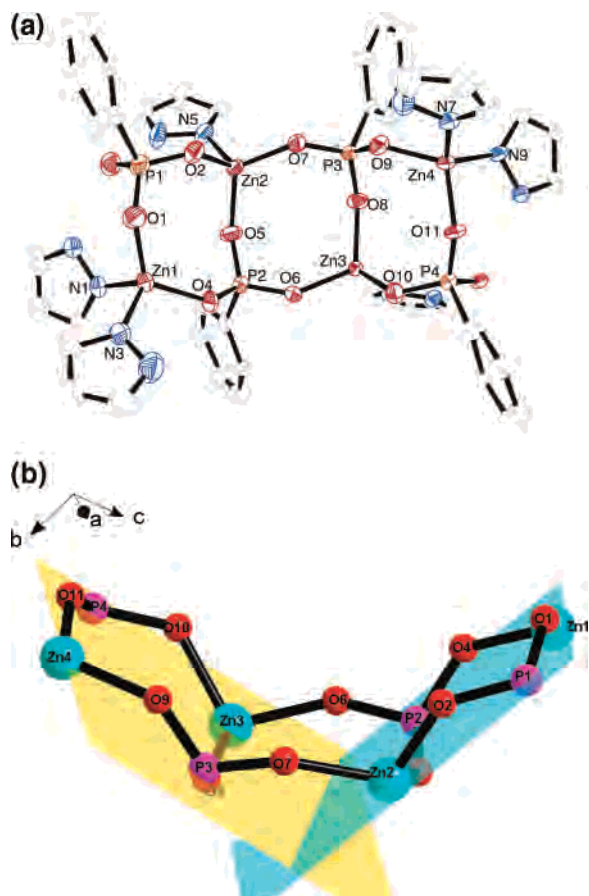


Figure 4. (a) ORTEP diagram of **4** (ellipsoids at 50% probability). The hydrogen atoms, the isopropyl substituents on the phenyl rings, the methyl substituents on the pyrazole rings, and solvent methanol molecules are not shown for clarity. Color scheme: Zn, dark-red; P, orange; O, red; N, blue; C, gray. (b) The core structure of **4**. The dihedral angle (77°) between two mean-planes of adjacent eight-membered rings of **4** is shown. Color scheme: Zn, green; P, pink; O, red; C, gray.

open-book conformation. The tricyclic structure is made up of three fused eight-membered rings where the four phosphonate ligands assist in the assembly of **4** (Figure 4). Two of these phosphonates (P2 and P3) act as tridentate $[\text{ArPO}_3]^{2-}$ ligands and function to bridge three zinc atoms (phosphonate (P2) bridges Zn2, Zn3, and Zn4, while phosphonate (P3) bridges Zn1, Zn2, and Zn3). The two other phosphonate

ligands present in **4** are bidentate $[\text{ArP}(\text{OH})(\text{O})_2]^-$ (P1 and P4) and bridge the terminal zinc atoms. In these terminal phosphonate ligands the P–OH remains free. As described above the two phosphonate ligands are discriminated by the ^{31}P NMR in solution. All the zinc atoms in **4** are tetra-coordinate. While the terminal zinc atoms (Zn1 and Zn4) have a 2N,2O coordination, the central zinc atoms (Zn2 and Zn3) have a 1N,3O coordination. Another slight variation occurs in the nature of the coordinating pyrazole ligands. Unlike in the case of **3**, in this case, two of the pyrazoles are deprotonated and function as anionic ligands. These are bound to the central zinc atoms. Each of the three eight-membered rings present in **4** is puckered with the oxygen atoms being displaced from the mean plane considerably. The dihedral angle between the successive eight-membered rings is about 77° . The open-book conformation of **4** suggests that this compound can be further folded into a cage by proper ligand design. Alternatively, polymeric sheets of fused eight-membered rings resembling one-dimensional zinc phosphate structures^{4d} also seem likely. The steric role of the $\text{ArP}(\text{O})(\text{OH})_2$ in restricting the cluster size to four becomes evident in comparison with the formation of the hexanuclear zinc(II) phosphonate, $[\text{Zn}_6\text{Cl}_4(\text{DMPZH})_8(\text{PhPO}_3)_4]$ (Chart 2), where the sterically unencumbered phenyl phosphonic acid is used.^{4b} On the other hand, the use of *tert*-butylphosphonic acid limits the cluster size to only three^{4b} (Chart 2).

In conclusion, we demonstrate the utility of a sterically hindered lipophilic phosphonic acid $\text{ArP}(\text{O})(\text{OH})_2$ in a three-component reaction involving the ancillary pyrazole ligands for the synthesis of metallophosphonates. Despite the multi-component nature of the reaction the product yields are very high. The lipophilicity of the phosphonic acid and the pyrazole ligands ensures the solubility of the multimetallic phosphonates in normal organic solvents. This synthetic methodology is potentially very versatile and can be used to prepare structurally diverse metallophosphonates. Studies in this direction are in progress in our laboratory.

Acknowledgment. V.C. thanks the Department of Science and Technology, India, and the Council of Scientific and Industrial Research, India, for financial support. P.S. thanks the Council of Scientific and Industrial Research, India, for the award of a Senior Research Fellowship. We are also thankful to the Department of Science and Technology, New Delhi, India, for funding the National Single-Crystal X-ray Facility at the Indian Institute of Technology, Kanpur, India.

Supporting Information Available: Figures S1 and S2 showing ORTEP diagrams of compounds **1** and **2**, Figure S3 showing the UV–vis spectrum of **3**, Figures S4 and S5 showing the TGA traces of **3** and **4**, Figures S6–S9 showing the infrared spectra of compounds **2**–**4**, Table S1 listing the mean-plane information on **1**, Tables S2–S5 giving the bond length and angle data for **3** and **4**, and crystallographic data in CIF format. This material is available free of charge via the Internet at <http://pubs.acs.org>.

IC060003Y